



# Heat release process in three-dimensional macro-cellular SiC reactor under Diesel engine-like conditions

J. Cypris<sup>b,1</sup>, L. Schlier<sup>a</sup>, N. Travitzky<sup>a</sup>, P. Greil<sup>a</sup>, M. Weclas<sup>b,\*</sup>

<sup>a</sup> University of Erlangen–Nuremberg, Department of Materials Science, Martensstr. 5, D-91058 Erlangen, Germany

<sup>b</sup> University of Applied Sciences Nuremberg, Department of Mechanical Engineering, Kesslerplatz 12, D-90489 Nuremberg, Germany

## HIGHLIGHTS

- Combustion reactor heat capacity significantly influences the thermodynamics of the process.
- Low- and high-temperature oxidation in a porous reactor is much faster with shorter delay time.
- Combustion temperature and pressure peaks are significantly reduced in porous reactor.
- Qualitative similarity of heat release process under Diesel and in porous reactor conditions.

## ARTICLE INFO

### Article history:

Received 18 September 2010

Received in revised form 17 May 2012

Accepted 23 May 2012

Available online 6 June 2012

### Keywords:

Combustion in porous reactors  
Clean flameless combustion under pressure  
Diesel injection  
Three dimensional printing  
Macro-cellular silicon carbide

## ABSTRACT

A specially developed macro-cellular SiC non-foam reactor has been used for investigations into Diesel-fuel injection, mixture formation and the heat release process inside a porous structure under piston-engine conditions. The heat release process has been compared to a free Diesel combustion indicating a significant influence of the reactor heat capacity on the thermodynamics of the process. Generally, the low- and high-temperature oxidation processes in a porous reactor are much faster, because of shorter delay time as compared to a free non-premixed combustion. High heat capacity of the porous reactor as compared to the gas heat capacity results in significantly reduced combustion temperature and corresponding combustion pressure peaks. Foam reactors with low and high pore density have also been compared in this investigation. The mixture formation, heat transfer and heat release processes performed in a porous reactor are very complex and depend on a number of different parameters of the combustion reactor in question: reactor structure, its heat capacity, pore size, specific surface area and wall junction geometry. Distribution of characteristic regions plotted in  $p$ – $T$  areas indicates qualitative similarity of heat release process as performed under Diesel-like and in porous reactor conditions.

© 2012 Elsevier Ltd. All rights reserved.

## 1. Introduction

Fuel injection, mixture preparation, low- and high-temperature oxidation processes (including ignition) play a critical role in the control of an engine combustion process, especially in the case of a self-ignition process, and corresponding exhaust emissions. The low-temperature oxidation is usually treated as a two-stage process: cool and blue flames are followed by high-temperature oxidation. The time between the beginning of fuel injection and the rapid pressure increase corresponding to the high-temperature heat release process is considered as an ignition delay period. During this period a number of complex chemical and physical processes have to be performed. For example chemical reactions (so-called

pre-ignition or low-temperature oxidation processes) are performed in order to prepare proper conditions for a thermal ignition (auto ignition) process in dependence on the temperature and pressure conditions. Physics of the process must consider a chain of such processes as the fuel supply process (injection), spray distribution in space, spray atomization, fuel vaporization and mixing with air. These processes are of high complexity especially in the case of Diesel-like engine conditions where the resulting mixture is highly non-homogeneous and time–space dependent. For a future clean engine (required homogeneous combustion) the chemistry of the pre-ignition processes as well as controlled auto ignition are the key factors for process realization under variable engine loads and rates. Further engine development requires the realization of a combustion process fulfilling the following conditions: lowest fuel consumption (minimum CO<sub>2</sub>) and nearly-zero exhaust emissions level. Both requirements can only be satisfied by the realization of a homogeneous combustion process. This process is here defined

\* Corresponding author. Tel.: +49 91158801898; fax: +49 91158805710.

E-mail address: [mirosław.weclas@ohm-hochschule.de](mailto:mirosław.weclas@ohm-hochschule.de) (M. Weclas).

<sup>1</sup> Present address: Fraunhofer Institute for Building Physics, Stuttgart, Germany.

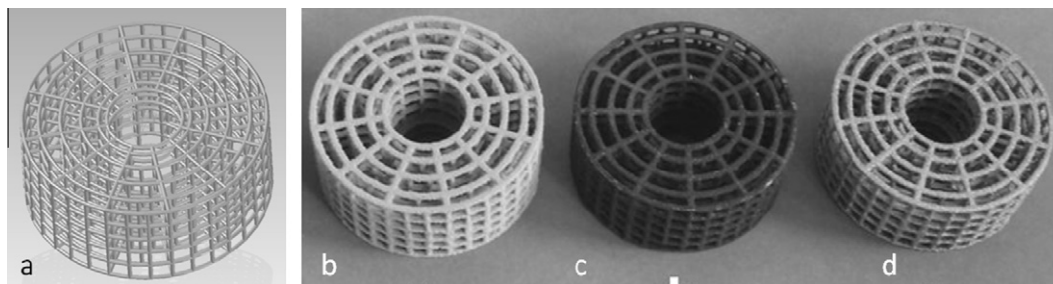


**Fig. 1.** (a) Model lattice structure for three-dimensional printing; macro-cellular structures manufactured by 3D printing: (b) as-printed and liquid silicone resin infiltrated, (c) pyrolysed and (d) Si infiltrated (SiSiC).

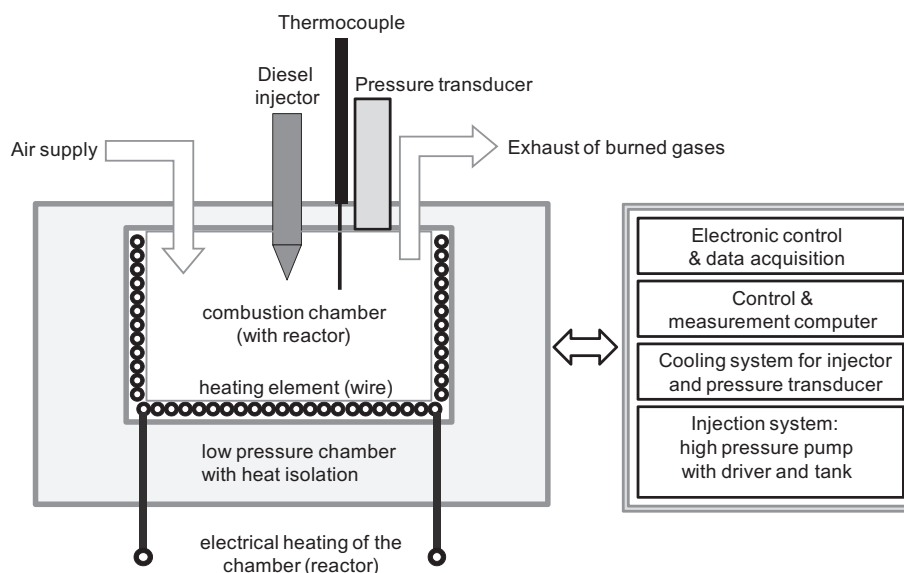


**Fig. 2.** Scheme of the test rig with combustion chamber.

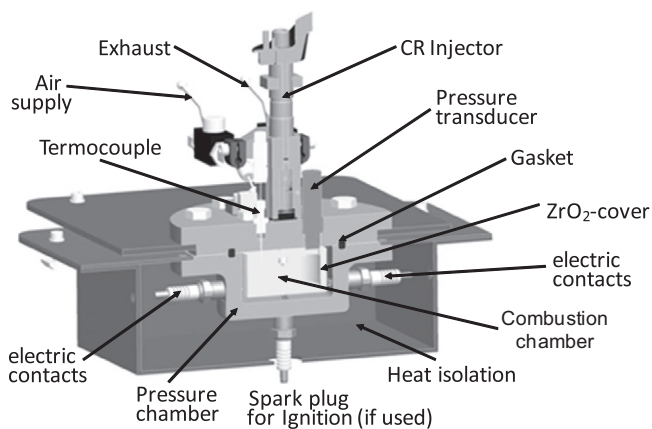


**Fig. 3.** Cross-section of combustion chamber.

as a simultaneous volumetric ignition of a homogeneous (preferably premixed) mixture. As a result a flameless combustion process characterized by a homogeneous temperature field is expected. Application of such a kind of combustion requires not only homogenization of the charge in a wide range of engine loads, but control of ignition timing at variable mixture compositions ( $\lambda$ ) and engine speeds, control of the heat release rate and corresponding cylinder pressure and pressure gradient, as well as control of the combustion

temperature for very low  $\text{NO}_x$ -levels. There is a number of engine concepts (mostly known as a HCCI systems), but no system known to the authors can satisfy all conditions selected above, at least if variable load conditions are considered. There are also “unconventional” engine concepts having a great potential for realization of a homogeneous combustion process in engines. One of such engine concepts is of an engine in which mixture formation, ignition and combustion processes are performed not in a free volume of combustion chamber but in a porous reactor, as proposed by Durst and Weclas [1]. This engine concept has great potential for high cycle efficiencies and for a nearly-zero emissions level allowing combustion temperature control below thermal  $\text{NO}_x$ -formation. There is only very weak information available in the literature on this kind of combustion in engines. Especially there is a lack of information on the nature of actual processes in porous reactors. Additionally, development of a high-temperature open cell and highly porous structures for application to internal combustion engines is necessary for development of this kind of combustion systems. The present paper combines both the development of three-dimensional open-cell macro-cellular non-foam structures with basic investigation on mixture formation and combustion in such reactors under engine-like conditions. For realization of engine combustion in a porous reactor it is very important to understand the role of the reactor (especially its structure and heat capacity) in supporting of engine processes such as fuel distribution in space, fuel vaporization and charge homogenization as well as heat release.

**Table 1**

Definition of different delay times of pre-ignition and high-temperature oxidation reactions.

Symbol	Name	Definition
$t_{CF}$	Characteristic time of cool-flame reactions	Time period between start of fuel injection (IB) and the beginning of cool-flame pre-ignition reactions
$t_{BF}$	Characteristic time of blue-flame reactions	Time period between start of fuel injection (IB) and the beginning of blue-flame pre-ignition reactions
$t_{comb}$	Characteristic time of high-temperature reactions	Time period between start of fuel injection (IB) and the beginning of high-temperature oxidation reactions (thermal ignition)

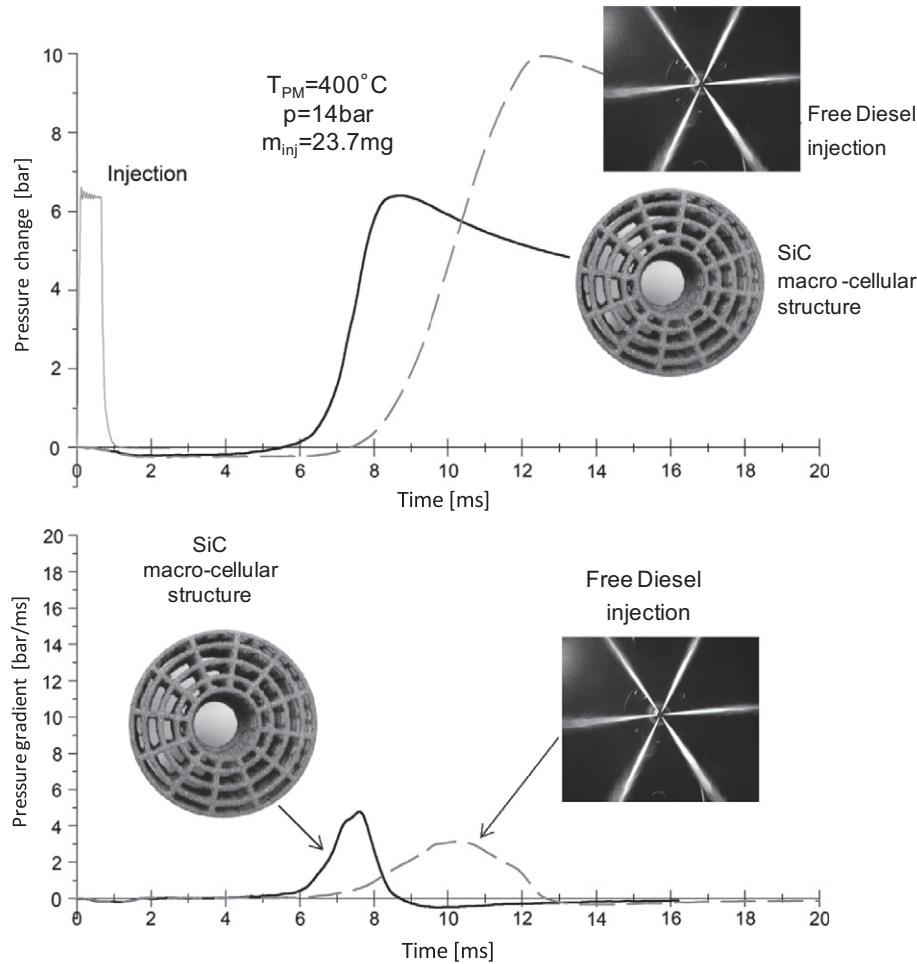


**Fig. 4.** Heat-release process in a porous reactor (SiC macro-cellular structure) as compared to free Diesel-like combustion;  $p_{IB} = 14$  bar,  $T_{IB} = 400$  °C,  $p_{inj} = 600$  bar,  $m_{fuel} = 23.7$  mg.

The present paper describes a unique experimental investigation, probably one of the first reported in the literature, on combustion in open-cell macro-cellular reactors under Diesel-engine-like conditions. Section 2 describes a macro-cellular reactor with a combustion chamber and under test conditions as used in the present investigation. Section 3 describes results and their discussion. In Subsection 4.1 the heat release process in a macro-cellular SiC reactor is compared to a free Diesel-like combustion process. Additionally, the process is compared to combustion in porous reactors made of SiC foam structures having different pore densities. Subsection 4.2 describes the heat-release process in a macro-cellular SiC non-foam reactor for different test conditions: at constant reactor temperatures and variable initial gas pressures, as well as for a constant amount of injected fuel. Results are summarized in Section 5.

## 2. Combustion reactors, combustion chamber and test conditions

### 2.1. Macro-cellular SiC non-foam porous reactor

SiC ceramics have been a focus of attention in the field of porous ceramics due to their superior properties at high temperatures, such as high thermal conductivity, excellent corrosion and oxidation resistance, and good thermal shock and thermal fatigue stability [2–4]. Although SiC and SiSiC ceramics start to oxidize at temperatures as low as 600 °C, a dense protection layer of amorphous silica is formed on the surface which allows these materials to be used up to reasonably high temperatures. Compared to alumina, Si-infiltrated reaction-bonded SiC (RB-SiSiC) has the benefits of a high thermal conductivity and emissivity, a

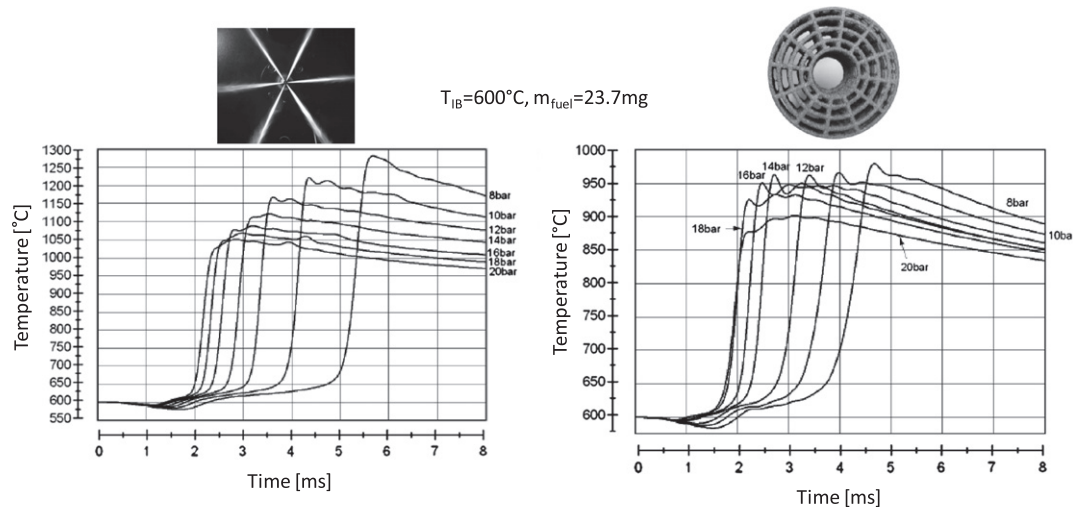


Fig. 5. Temperature histories of heat release process in free volume combustion chamber and in macro-cellular reactor at initial temperature  $T_{IB} = 600^\circ\text{C}$  and  $m_{\text{fuel}} = 23.7\text{ mg}$ .

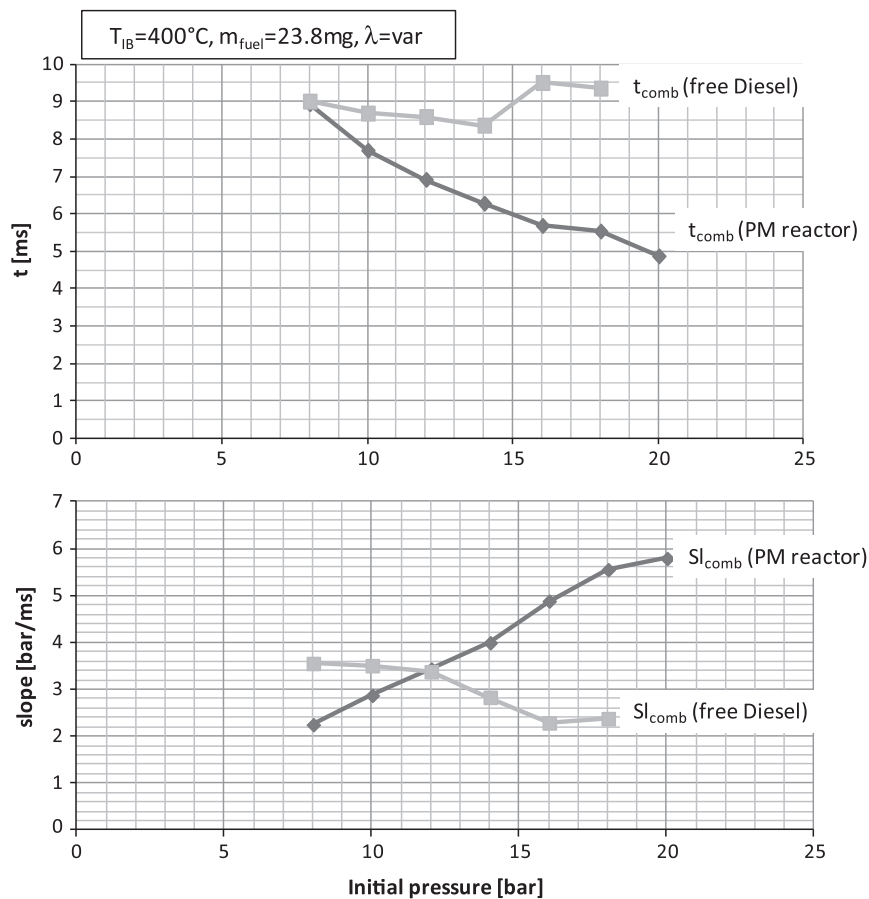


Fig. 6. Delay time  $t$  and reaction rate (slope  $sl$ ) in a porous reactor (SiC macro-cellular structure) as compared to free Diesel-like combustion;  $T_{IB} = 400^\circ\text{C}$ ,  $p_{inj} = 600\text{ bar}$ ,  $m_{\text{fuel}} = 23.8\text{ mg}$ .

lower coefficient of thermal expansion, and very good thermal shock resistance [5–7]. For the present investigations a macro-cellular lattice structure based on silicon carbide (non-foam structure) with 600 vertical cylindrical struts was fabricated and applied to engine-like combustion conditions (Fig. 1). The lattice design with a high porosity >80% was shaped by indirect three-dimensional printing of a SiC powder mixed with a dextrin binder which also serves as a carbon precursor. Pressureless infiltration

of silicon melt at  $1500^\circ\text{C}$  driven by capillary suction finally resulted in dense struts of reaction bonded silicon carbide composed of approximately 50 wt.% SiC and 50 wt.% Si. Fig. 1 shows the macro-cellular structures at the various stages of processing. Total dimensional changes of <3% during the whole processing stage were measured. An experimental procedure for manufacturing of the macro-cellular lattice structure has been described in detail in [8].



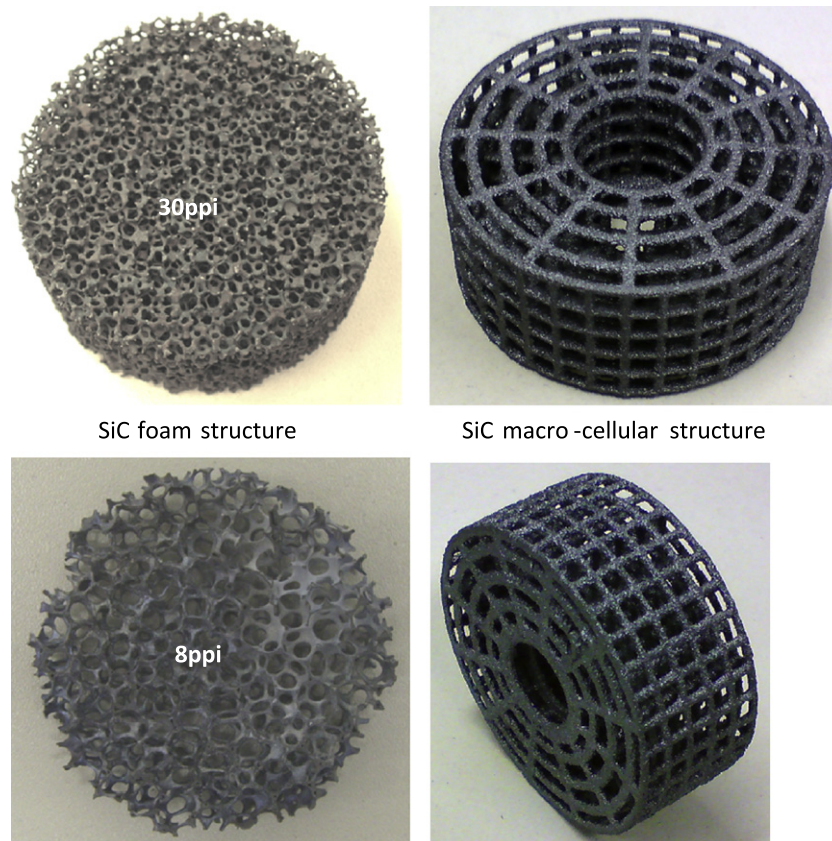


Fig. 7. Comparison of SiC foam reactor (left) and macro-cellular SiC non-foam reactor (right).

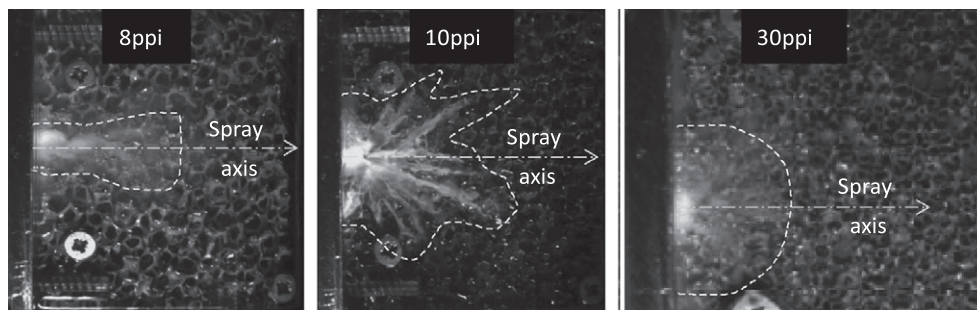


Fig. 8. Comparison of fuel distribution over the reactor cross-section during Diesel injection for reactors having different pore densities (8 ppi, 10 ppi and 30 ppi).

## 2.2. Combustion chamber and fuel injection system

In order to perform detailed investigations on low- and high-temperature oxidation processes in porous reactors under engine-like conditions of wide flexibility, a special high-pressure, high-temperature, constant-volume and adiabatic combustion chamber has been built and equipped with a Diesel common-rail injection system (Figs. 2 and 3).

This system simulates the thermodynamic conditions at the time instance of injection onset (corresponding to the nearly TDC of compression in a real engine), however, the pressure and temperature can be chosen independently from one another [9–11].

The following test conditions characterize the variability of the combustion chamber used in the present investigation:

- free setting of initial chamber temperature in the range from 20 °C to 1000 °C
- free setting of the initial chamber pressure in the range from 1 bar to 20 bar
- insulation of the thermal radiation of the chamber walls
- different CR injectors can be used and variable injection parameters can be applied (injection pressure, duration, multiple injection, etc.)
- CR injector is water cooled preventing thermal overload in the chamber
- conventional spark plug is applied for simulation of local ignition (if applied)
- controlled amount of air (or gas) supply for control of air-excess ratio
- variable vertical location of the nozzle tip in the chamber
- combustion chamber is covered with thermally insulated external chamber
- chamber temperature is set using an electrical heating system (electric contacts through electrodes of conventional spark plugs)

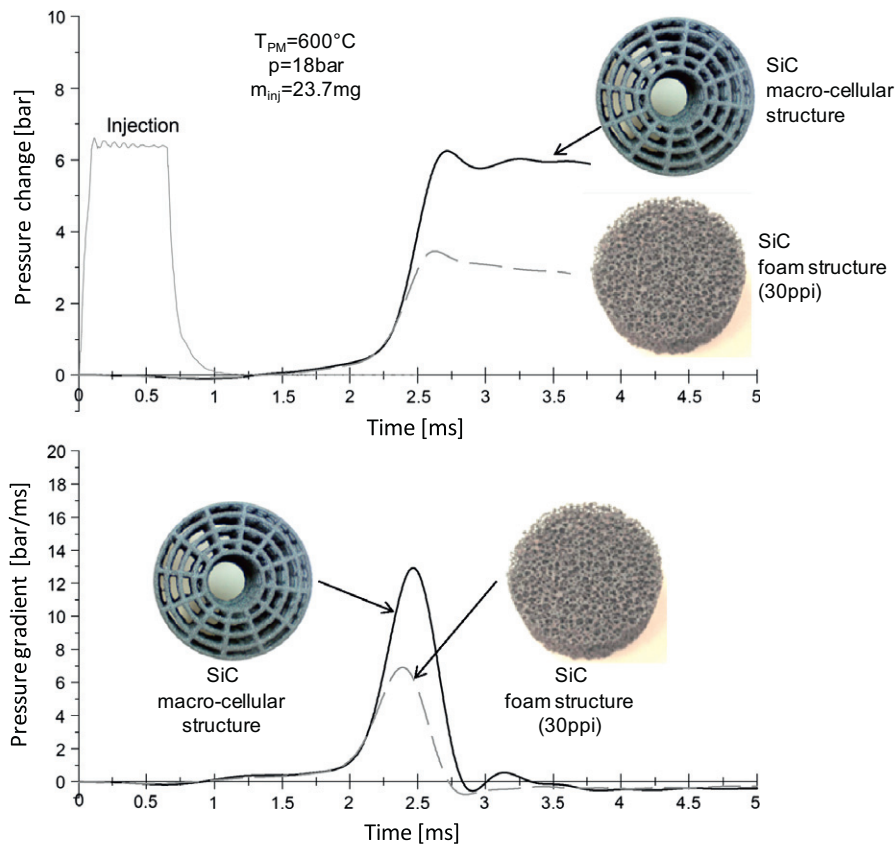


**Fig. 9.** Comparison of pressure histories (top) and pressure gradients (bottom) of the combustion process in a macro-cellular SiC reactor with combustion in a SiC-foam reactor of high pore density (30 ppi) for initial temperature  $T_{IB} = 600^\circ\text{C}$  and initial gas pressure  $p_{IB} = 18\text{ bar}$ ,  $m_{fuel} = 23.7\text{ mg}$  (pressure traces are measured in time after fuel injection starts).

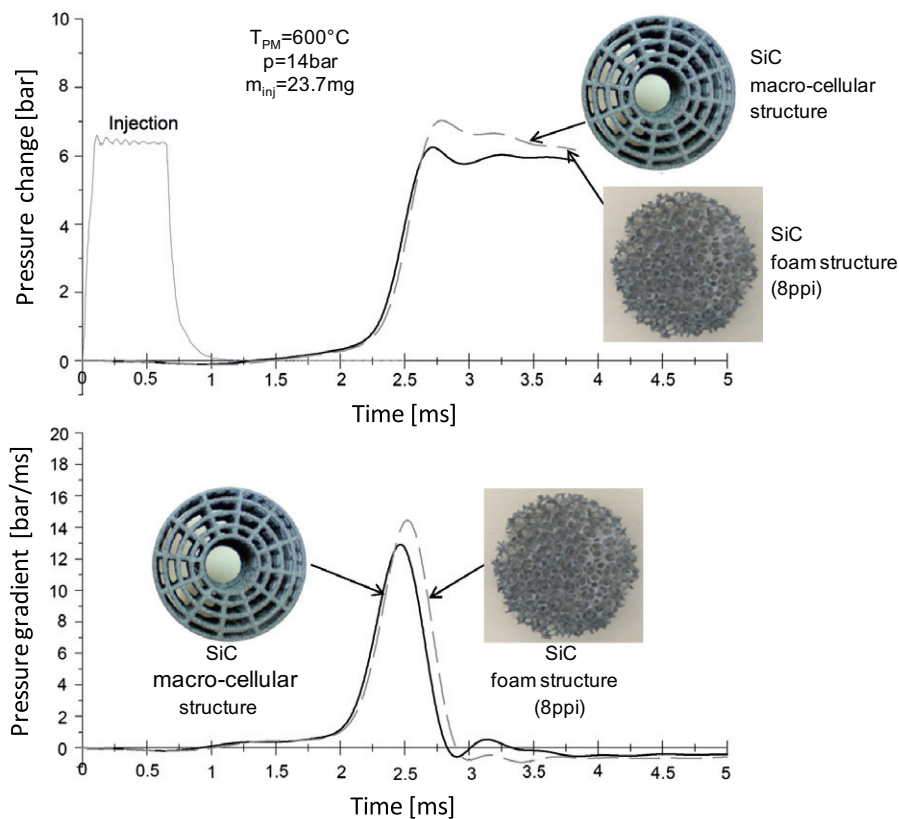


**Fig. 10.** Comparison of pressure histories (top) and pressure gradients (bottom) of the combustion process in a macro-cellular SiC reactor with combustion in a SiC-foam reactor of low pore density (8 ppi) for initial temperature  $T_{IB} = 600^\circ\text{C}$  and initial gas pressure  $p_{IB} = 14\text{ bar}$ ,  $m_{fuel} = 23.7\text{ mg}$  (pressure traces are measured in time after fuel injection starts).

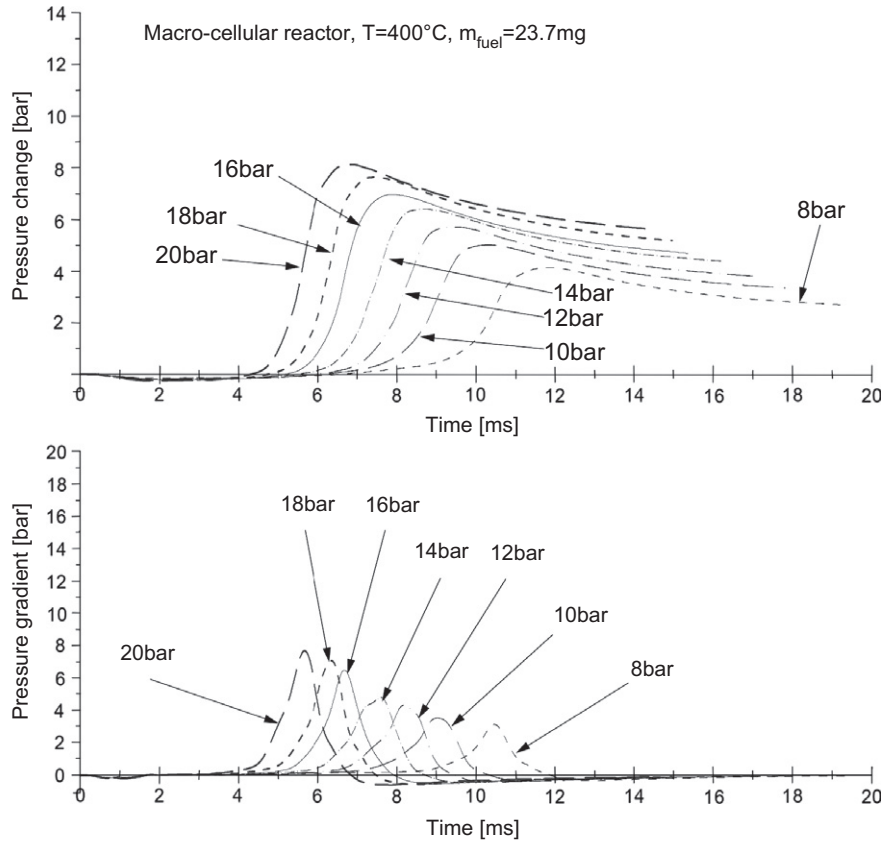


**Fig. 11.** Pressure history (top) and pressure gradient distribution (bottom) as measured in a macro-cellular SiC non-foam reactor in time after fuel injection starts:  $T_{\text{IB}} = 400^{\circ}\text{C}$ ,  $m_{\text{fuel}} = 23.7\text{ mg}$ ,  $p_{\text{IB}} = \text{var}$ .

- combustion chamber is equipped with a high-resolution pressure transducer for measuring pressure history
- combustion chamber can additionally be equipped with an endoscopic visualization system including a CCD or a high-speed camera.

During the combustion process the chamber is considered as a closed system having a constant volume. According to the first law of thermodynamics for a constant-volume and adiabatic system the changes in the internal energy  $du/dt$  directly correspond to the heat release rate in the chamber  $dQ/dt$ . Assuming that the combustion chamber during a short period of ignition and combustion is considered as an adiabatic system, any measured changes in the chamber pressure correspond directly to the heat released (or consumed) in the chamber.

### 3. Test conditions for investigating of Diesel injection and combustion in porous structures

A non-stationary flameless and clean combustion under piston engine conditions as performed in porous structures include a number of individual processes including high pressure fuel injection, fuel distribution in the reactor volume, heat transfer, fuel vaporization, pre-ignition reactions (cool and blue flames), thermal ignition and combustion process itself [9–11]. The nature of these processes is still almost unknown and only very weak information is available in the literature. Especially a lack of experimental data is noticeable. Basic research and measurements on individual processes in porous reactors as presented in this paper have been performed in special measurement systems for investigating

high-pressure Diesel injection and fuel distribution in porous structures [12–16], as well in a combustion chamber as described above. The process of fuel distribution in a porous reactor has been investigated using CCD and high-speed visualization techniques under atmospheric thermodynamic conditions. In the case of combustion process chamber pressure and pressure gradient histories measured during the time after the onset of Diesel injection are measured and analysed [9–11].

For process analysis a phenomenological model of a multi-step oxidation (and ignition) has been constructed and used in the present analysis as described in [9–11]. In this model two measured parameters are investigated: pressure history and pressure gradient distribution both as a function of time after injection begins. The whole process is analysed from time “zero” defined as a trigger signal for Diesel injector (start of injection “IB”). At this point the thermodynamic conditions in the combustion chamber are characterized by initial chamber pressure  $p_{\text{IB}}$  and initial chamber temperature  $T_{\text{IB}}$ . Additionally, a characteristic time  $t$  (delay time) of a particular phase of the process is analysed and measured starting at zero-time point (point IB) – see Table 1. These characteristic time instances are measured at locations of particular points with respect to the zero time-line;  $t_{\text{CF}}$  is the characteristic time of cool-flame reactions;  $t_{\text{BF}}$  is the characteristic time of blue-flame reactions;  $t_{\text{comb}}$  is the characteristic time of high-temperature reactions. For analysis of the reaction rate a slope of the reaction curve corresponding to the particular oxidation process is described by average pressure changes in time [bar/ms];  $sl_{\text{CF}}$  is the slope of cool-flame reactions;  $sl_{\text{BF}}$  is the slope of blue-flame reactions;  $sl_{\text{comb}}$  is the slope of high-temperature oxidation (heat release).

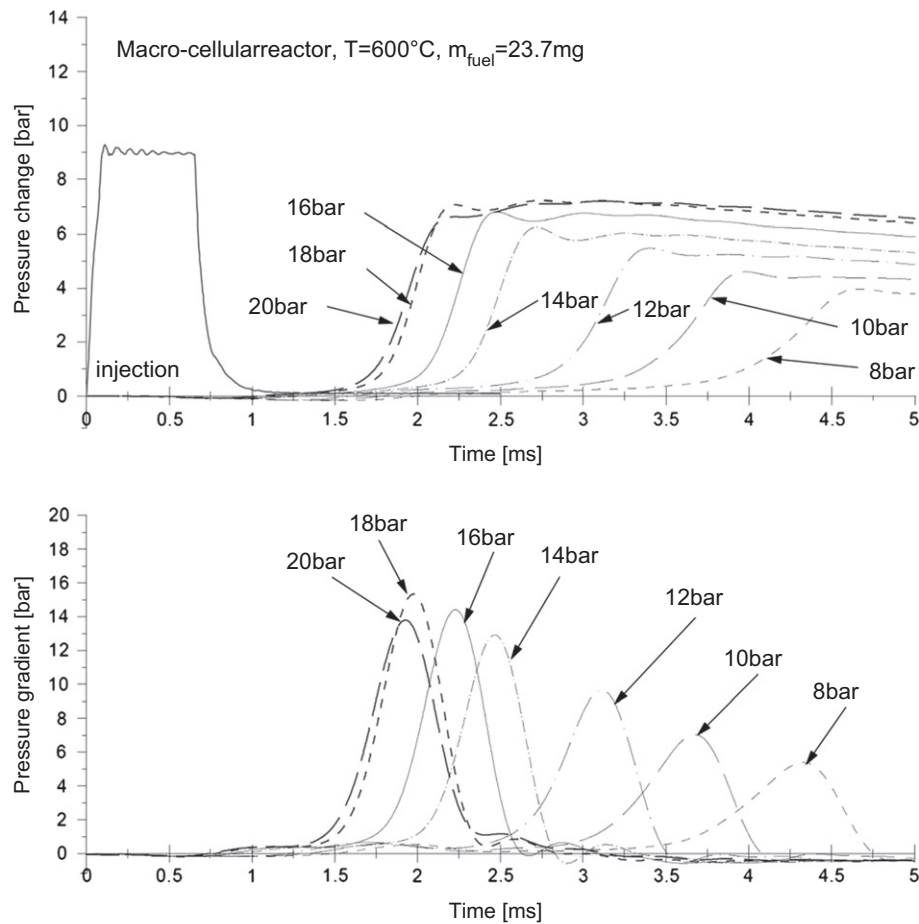


**Fig. 12.** Pressure history (top) and pressure gradient distribution (bottom) as measured in a macro-cellular SiC non-foam reactor in time after fuel injection starts:  $T_{\text{IB}} = 600^{\circ}\text{C}$ ,  $m_{\text{fuel}} = 23.7\text{ mg}$ ,  $p_{\text{IB}} = \text{var}$ .

## 4. Results and discussion

### 4.1. Comparison of processes in porous reactors and free volume

In order to underline significant differences in the heat-release process (combustion) in a porous reactor, this process will be compared to the free combustion in a gas phase. For this reason simple models of an adiabatic free volume and porous reactor have been developed as described below. The reactor consists of a constant-volume adiabatic combustion chamber filled with working gas. A given amount of energy  $E_{\text{ch}}$  is supplied with injected fuel into the chamber. As a result of oxidation processes (heat release) this energy is transferred into heat  $Q_{\text{in}}$ . According to this heat release  $Q_{\text{in}}$  the internal energy of the gas increases and the gas temperature changes according to the internal energy change. In a constant-volume and adiabatic combustion chamber this results in chamber pressure changes  $\Delta p$  corresponding to the gas temperature changes  $\Delta T$ . In the case of a non-stationary process a pressure history in time is investigated. In the case of a porous reactor the system consists of a porous reactor (PM) and working gas trapped in the reactor volume. The system has a constant volume and is an adiabatic combustion chamber completely filled with the porous structure. Again a given amount of energy  $E_{\text{ch}}$  is supplied with fuel injection into the reactor free volume (open pores volume). As a result of oxidation processes this energy will transfer into heat  $Q_{\text{in}}$ . This heat release increases the internal energy of the gas trapped in the porous structure volume and of the reactor itself. According

to this energy increase the gas temperature changes according to the internal energy change including energy change of the porous reactor [17]. Contrary to the free-volume reactor, the gas trapped in a porous reactor volume cannot be thermodynamically decoupled from the internal energy changes of the reactor. Additionally it must be considered that the mass of the porous reactor is at least hundreds of times higher than the mass of gas trapped inside the PM volume. As a consequence of this thermal coupling of both "components", quite a different change in the gas temperature trapped in the PM volume results as compared to a free-volume reactor. Finally, a significantly reduced pressure change  $\Delta p$  is measured as a result of the combustion process in the porous reactor as compared to free-gas adiabatic conditions. This effect may clearly be observed in Fig. 4 comparing the heat-release process in a macro-cellular SiC structure with free Diesel-like combustion under initial pressure  $p_{\text{IB}} = 14\text{ bar}$  and initial temperature  $T_{\text{IB}} = 400^{\circ}\text{C}$ . Especially low-temperature oxidation processes (cool- and blue-flames reactions) are significantly accelerated in a porous reactor. The heat released in a high-temperature oxidation process (combustion) in the case of this reactor is partly transferred to the reactor solid phase making use of the larger heat capacity of this material as compared to the gas. These differences to free Diesel combustion are especially visible at lower initial temperatures  $T_{\text{IB}}$ . Especially important feature of combustion in reactor is reduced combustion temperature into its large heat capacity, as indicated in Fig. 5. This figure compares temperature histories as measured after fuel injection starts in free volume combustion



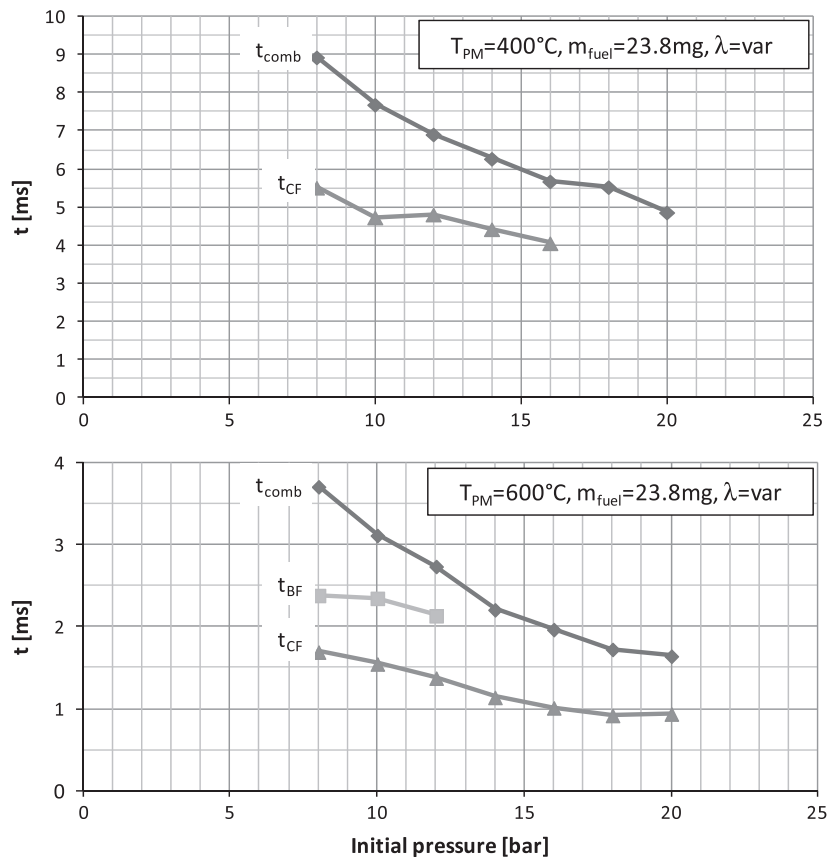


**Fig. 13.** Delay time as a function of initial chamber pressure measured at two initial reactor temperatures (400 °C and 600 °C) for a constant amount of injected fuel and variable air excess ratio.

chamber and in macro-cellular SiC reactor. Varying maximum temperature in a free volume combustion systems is due to variable air excess ratio corresponding to different initial conditions (initial pressure). Contrary to that, almost constant maximum combustion temperature in real porous reactor has been recorded independently of initial pressure indicates the role of heat capacity and heat transfer conditions defining amount of heat accumulated in the porous reactors.

Comparison of delay times ( $t$ ) and slopes ( $sl$ ) at relatively low initial temperature  $T_{IB} = 400$  °C is given in Fig. 6 (for definition see Table 1). The delay time is much shorter in a porous reactor as compared to free Diesel combustion. This is a result of energy accumulated in the reactor solid phase and very fast heat transfer inside the reactor volume. The reaction slope (reaction rate) in the porous reactor steadily increases due to the increase of initial pressure being much higher than for free Diesel combustion at high pressures  $p_{IB}$ . Please note that in both cases investigated, non-pre-mixed conditions are considered. This means that only the initial phase of the combustion process is considered. However, owing to the Diesel spray's interaction with a porous structure [12–16], the mixture inside the SiC reactor is better distributed in space as it is in the case of free Diesel injection. The pressure gradient history indicates that the heat release rate in a porous reactor is much higher than that of free Diesel combustion. The lowered combustion pressure peak is a result of lowered combustion temperature due to the heat capacity of the porous reactor. Consequently this effect leads to significantly reduced  $NO_x$  combustion emissions. Keeping the reactor temperature below thermal  $NO_x$ -formation, it is possible to realize a nearly-zero  $NO_x$  emissions level combustion process. The effect of a porous reactor on the mixture formation and combustion process is related to two main aspects:

as already indicated, heat capacity of the reactor and corresponding heat accumulation, and reactor structure significantly influencing the fuel injection process, fuel distribution in the reactor volume, fuel vaporization and mixing with air trapped in the reactor volume. From this point of view there is a number of parameters of a porous reactor which are critical when applied to the combustion process: pore size (cells), pore structure, pore density, heat capacity (mass), specific surface area, number of wall junctions for interaction with Diesel sprays, thickness of wall junctions, micro-porosity, thermal and mechanical stability. From this point of view there are two groups of reactors with significantly different features: foam structures and macro-cellular non-foam reactors [8]. Fig. 7 shows a comparison of both kinds of reactors. In the case of foam structures two different pore densities (high density: 30 ppi and low density: 8 ppi) are presented. It can be seen that pore size and density will significantly influence the fuel-injection process inside the reactor, as indicated in Fig. 8. The contour lines indicate the fuel distribution in the cross-section of the reactor. In the reactor of low pore density (8 ppi) the pores are large and the number of wall junctions is low resulting in reduced radial spreading of the fuel and predominately axial penetration (along the spray axis) of the Diesel jet. With increasing pore density (10 ppi and 30 ppi) the axial fuel penetration in a porous reactor decreases and radial spreading increases [12–16]. In the case of the combustion process pore density influences not only the fuel distribution in porous structure but also the heat capacity of the reactor significantly, bearing on pressure and temperature histories. Comparison of foam structure reactor (especially of high pore density) and macro-cellular non-foam reactor indicates that the latter structure is characterized by the following features: lower heat capacity, much larger pores, non-homogeneous pore structure,

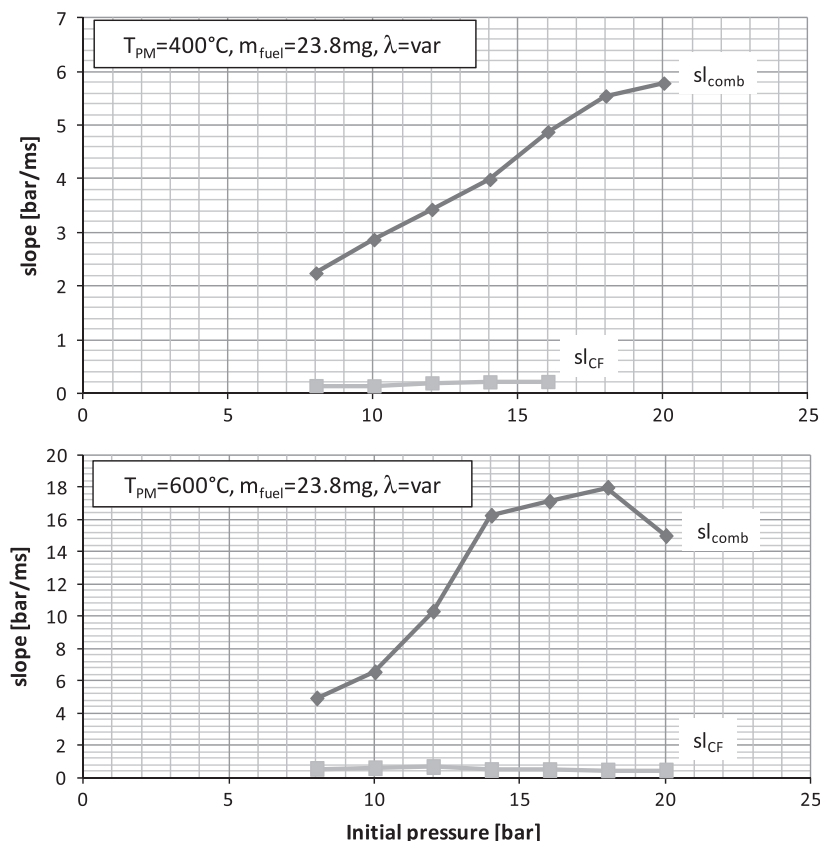


**Fig. 14.** Reaction slope as a function of initial chamber pressure measured at two initial reactor temperatures (400 °C and 600 °C) for a constant amount of injected fuel and variable air excess ratio.

much thicker wall junctions, fewer wall junctions, and much lower specific surface area. These differences are visible in the heat release process as measured in both kinds of reactor, see Fig. 9. This figure compares heat release processes in a macro-cellular reactor and in a foam-structure reactor of high pore density (30 ppi) under similar thermodynamic conditions. The low-temperature oxidation reactions (cool- and blue-flames reactions) perform similarly in either reactor. The heat-release process in a high-temperature oxidation process is different, especially owing to the differences in the heat capacity of either reactor. These differences are then significantly reduced by reducing the pore density of a foam reactor (8 ppi), as shown in Fig. 10. In this case the heat-release process, corresponding pressure history as well as heat-release rate are similar for both reactors; however, both reactors are characterized by significantly different pore size and pore structure. These examples indicate the complexity of mixture formation, auto-ignition and heat-release process as performed in porous reactors. Still no simple rules are known to understand the process, and intense investigations must be continued to describe the effect of different reactor parameters on the combustion process. The present investigation is an initial contribution to this topic.

#### 4.2. Heat release process in a macro-cellular SiC non-foam reactor

Experimental investigations on heat-release processes in a macro-cellular SiC non-foam reactor have been performed under different test conditions. In particular the effects of initial gas pressure  $p_{IB}$ , initial reactor temperature  $T_{IB}$  and the effect of the mass of injected fuel  $m_{fuel}$  on low- and high-temperature oxidation reactions including thermal (auto) ignition are considered. Pressure and pressure gradient histories as measured after

fuel injection starts in a porous reactor at  $T_{IB} = 400^\circ\text{C}$  and  $m_{fuel} = 23.7\text{mg}$  for different initial gas pressures  $p_{IB}$  are presented in Fig. 11. First insight into the pressure histories indicates that the gas pressure at the moment of fuel injection onset is a critical factor for the heat release-process (at constant initial temperature  $T_{IB}$ ). The higher the initial gas pressure  $p_{IB}$ , the shorter the delay time and faster the heat-release rate. The combustion pressure peak will go up with increasing initial chamber pressure. Pressure gradient distributions show a single-peak character indicating a single-step ignition process (or, that no ignition occurs). The maximum of pressure gradient distribution corresponds to the maximum of the heat-release rate.

At higher initial reactor temperature  $T_{IB} = 600^\circ\text{C}$  and variable initial gas pressure  $p_{IB}$  the investigated process is shown in Fig. 12. Similarly to the case of  $400^\circ\text{C}$ , the heat-release process is strongly pressure-dependent. At higher temperature ( $600^\circ\text{C}$ ), the delay time is significantly shorter as compared to the case of  $400^\circ\text{C}$ . At lower pressures ( $p_{IB} < 12\text{ bar}$ ) the reaction rate is much lower and the pressure history curves show very slow oxidation in an initial phase of the process. This low-temperature oxidation process is then significantly reduced at higher gas pressures. The pressure gradient shows that at initial gas pressures lower than 16 bar the distribution has a single-peak character indicating a single-step ignition process. At the highest pressure investigated, however, this character shows a tendency to be a bi-modal distribution indicating possible multi-step ignition conditions in the reactor. Delay times and reaction slopes for both initial temperatures investigated are plotted in Figs. 13 and 14. Firstly, a critical influence of the initial reactor temperature on delay time and reaction dynamics is observed. The delay times, both of low- and

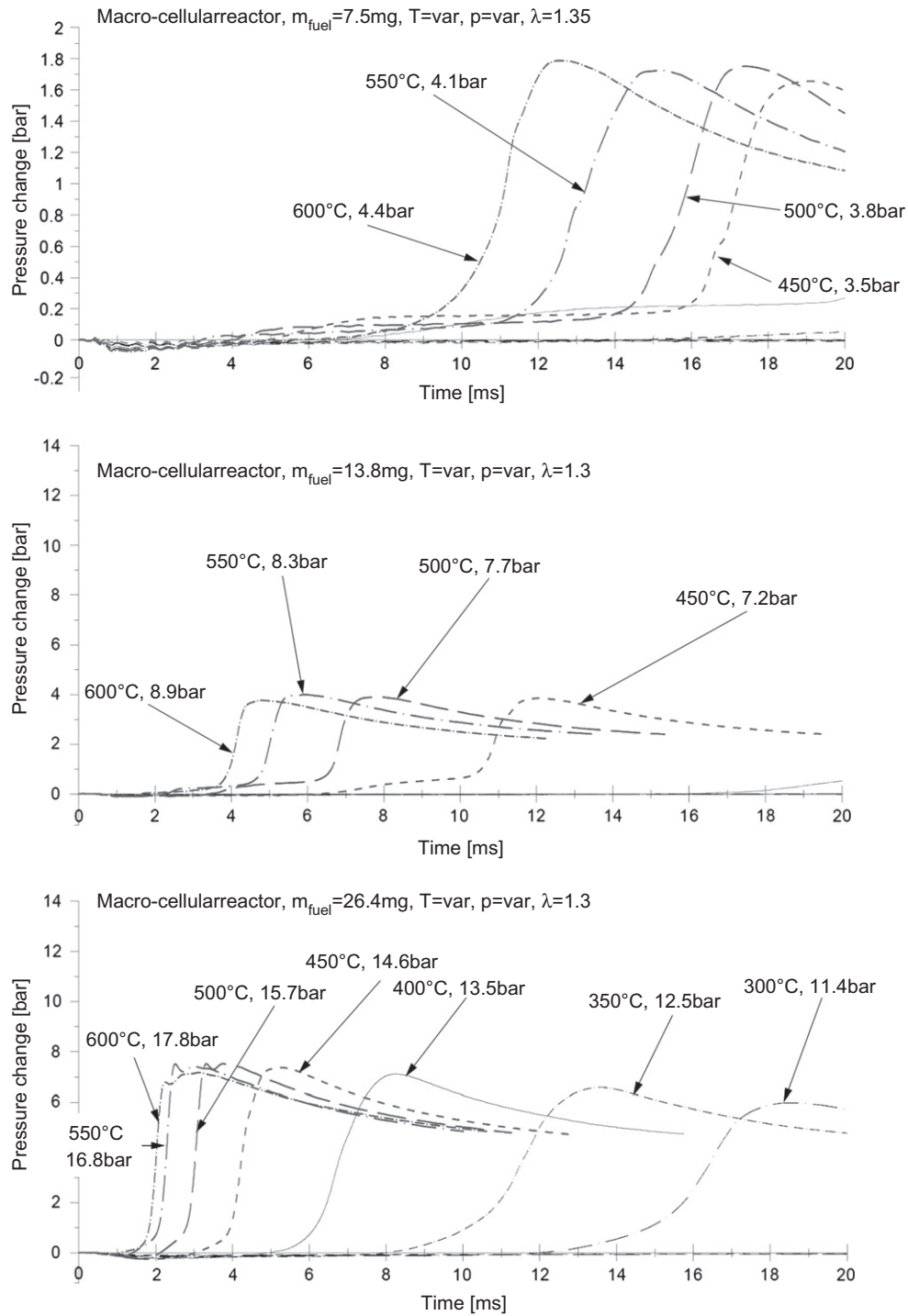


**Fig. 15.** Pressure history as measured in a macro-cellular SiC non-foam reactor in time after fuel injection starts at three constant amounts of injected fuel and constant air excess ratio ( $\lambda = 1.3$ ) for variable  $T_{IB}$  and  $p_{IB}$ : top –  $m_{fuel} = 7.5$  mg; middle –  $m_{fuel} = 13.8$  mg; bottom –  $m_{fuel} = 26.4$  mg.

high-temperature oxidation processes, gradually decrease with increasing initial chamber pressure  $p_{IB}$ . The reaction rate of a high-temperature process for initial reactor temperature 400 °C almost linearly increases with increasing initial chamber pressure from approximately 2 bar/ms at  $p_{IB} = 8$  bar to almost 6 bar/ms at  $p_{IB} = 20$  bar. The reaction rate of a low-temperature oxidation is significantly lower, being on the level of 0.2 bar/ms. At higher reactor temperature (600 °C) the behavior is similar, however, the slope for a high-temperature oxidation has a maximum at  $p_{IB} = 18$  bar. The reaction rates are two to three times higher than

those observed at lower reactor temperature. Again, the slope of low-temperature oxidation (cool-flame reactions) is low and almost 20 times lower than for a high-temperature process.

Finally, the process is investigated at constant mass of injected fuel and constant air excess ratio ( $\lambda$ ). Such test conditions require that the initial reactor temperature and initial gas pressure be variable. The heat-release process in a macro-cellular SiC reactor at three constant amounts of fuel injected into the reactor is shown in Fig. 15. The mass of injected fuel corresponds to the amount of energy supplied to the porous reactor. For a constant heat capacity

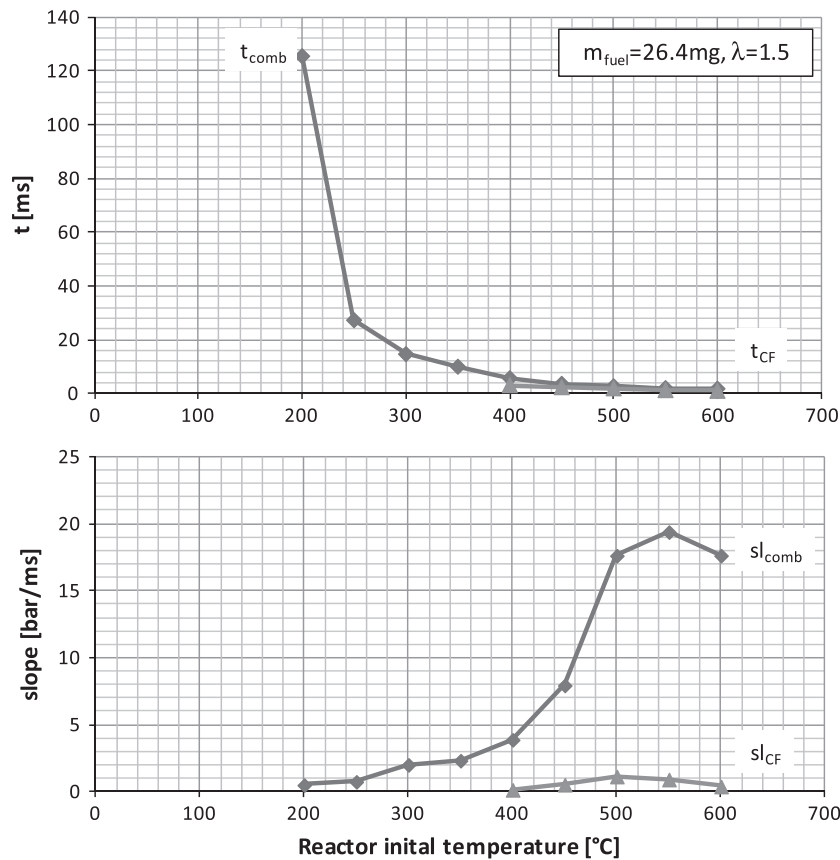


**Fig. 16.** Delay time (top) and reaction slope (bottom) distributions as functions of initial reactor temperature for a constant amount of injected fuel  $m_{\text{fuel}} = 26.4 \text{ mg}$  and constant air excess ratio  $\lambda = 1.5$ .

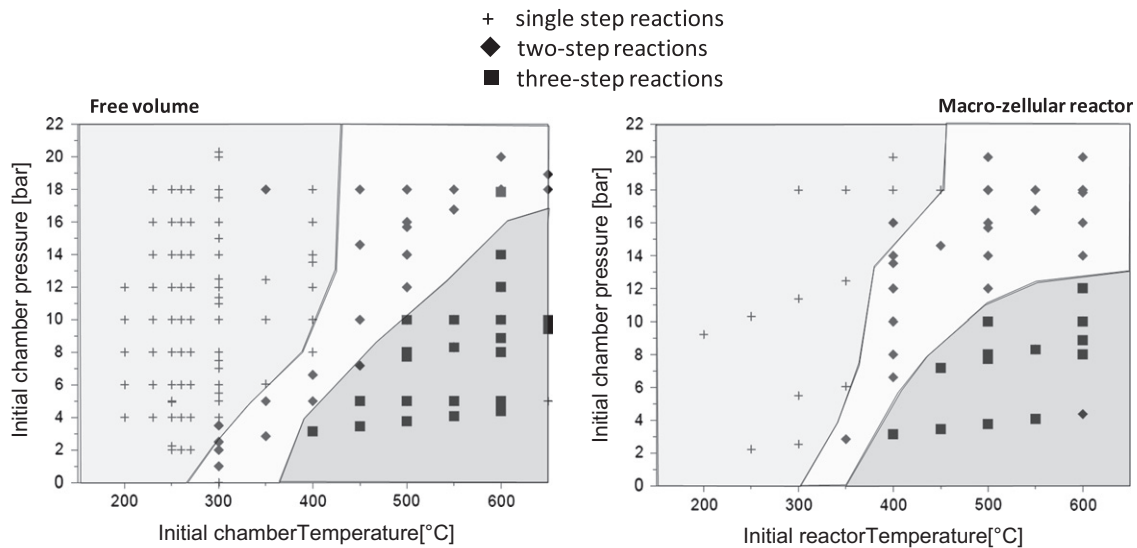


**Fig. 17.** Fields representing characteristic combustion modes in macro-cellular reactor as compared to free Diesel injection and combustion conditions.

of the porous reactor a variable amount of supplied energy  $E_{\text{ch}}$  (and corresponding heat  $Q$ ) means that different amounts of heat are accumulated in the reactor solid phase. Because of a very large reactor heat capacity as compared to the heat capacity of gas trapped in the porous medium volume, the reactor temperature changes will not directly follow the amount of released heat as would be expected in a free-volume system. This is clearly shown

in the case of a small amount of injected fuel ( $m_{\text{fuel}} = 7.5 \text{ mg}$ )—see top diagram in Fig. 15. There is only a weak increase of pressure after injection has started, indicating very low temperature increase of the gas in the reactor corresponding to the reactor temperature increase. With an increasing amount of injected fuel, more and more energy is supplied to the reactor, resulting in higher temperature change of the porous reactor. This temperature



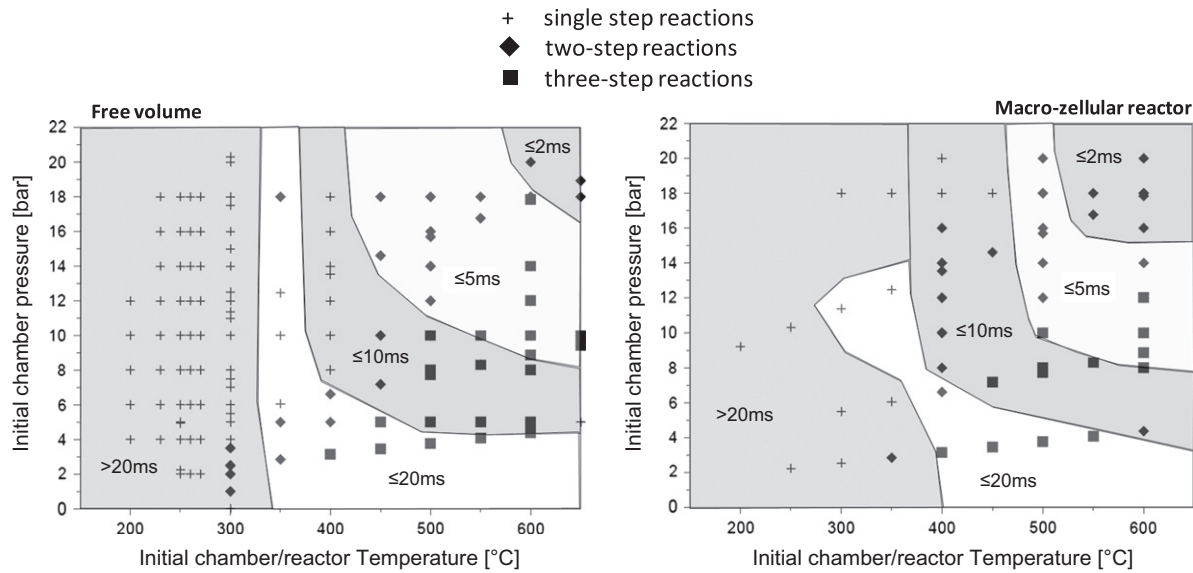


Fig. 18. Fields representing characteristic combustion modes and delay times in macro-cellular reactor as compared to free Diesel injection and combustion conditions.

change corresponds to the pressure change measured in the combustion chamber. An increasing amount of injected fuel significantly accelerates the low- and high-temperature oxidation processes and shortens delay time. At a small amount of injected fuel, a very much delayed and slow oxidation process is noticeable before chamber pressure rises. At larger amounts of injected fuel and at lower reactor temperatures, the process is significantly delayed due to lower reaction rates. With increasing reactor temperature, delay time is shortened and reaction rate (heat release) increases. At high reactor temperatures the heat-release process is very fast and performs very quickly after fuel injection starts. This is supported by analysis of delay time and reaction slope for a macro-cellular SiC non-foam reactor as a function of initial reactor temperature, as plotted in Fig. 16. At very low reactor temperatures the process is much delayed ( $t_{\text{comb}} > 120$  ms) and significantly accelerates with increasing temperature. At higher reactor temperatures, delay time is very short, on the level of 1 ms. Further increase of initial reactor temperature cannot considerably reduce this delay time. The reaction rate (slope distribution) significantly increases with increasing initial reactor temperature, especially for  $T_{\text{IB}} > 400$  °C. The slope has a maximum of distribution at  $T_{\text{IB}} = 550$  °C.

For an overall view of heat release performed in free volume and in macro-cellular reactor, characteristic features of the process have been plotted in  $p_{\text{IB}} - T_{\text{IB}}$  diagrams, as shown in Fig. 17. This diagram shows characteristic reaction behavior represented by a single- and multi-step oxidation [11]. There are three regions representing three different characteristics of the oxidation process: region 1 – single-step reactions and is located at lower initial temperatures for all initial pressures; region 2 – multi-step reactions with two slopes recognizable in the reaction curve and is located in the range of middle-high initial temperatures at middle-high initial pressures; region 3 is characterized by multi-step reactions with three slopes recognizable in the reaction curve and is located in the range of higher initial temperatures at low-middle initial pressures.

Another characteristic feature of investigated processes is reaction delay time, as shown in Fig. 18. There are five characteristic regions to be selected according to the delay time ( $t$ ) duration:  $t > 20$  ms located at lower initial temperatures at all investigated initial pressures;  $10 \text{ ms} < t \leq 20$  ms located at higher initial temperatures and lower initial pressures as well as in a small region of high initial pressures;  $5 \text{ ms} < t \leq 10$  ms located at higher initial

temperatures and lower-middle initial pressures as well as in a small region of high initial pressures;  $2 \text{ ms} < t \leq 5$  ms located at higher initial temperatures and middle to high initial pressures;  $t \leq 2$  ms and is located at high initial temperatures and high initial pressures. Analysis of characteristic regions presented in Figs. 17 and 18 indicates qualitative similarity of heat release process as performed under Diesel-like and in porous reactor conditions.

## 5. Concluding remarks

For conducting experimental investigations a unique macro-cellular SiC non-foam reactor has been developed and used for the investigation of Diesel-like fuel injection, mixture formation and heat-release process under piston-engine conditions. A special constant-volume and adiabatic combustion chamber has been used for simulation of piston-engine conditions.

Using a common-rail Diesel injection system, fuel was injected into the porous reactor and the following processes of fuel distribution, vaporization, mixing with air, thermal auto-ignition and heat release were performed in the reactor volume. A high-pressure Diesel injection process was realized in such a structure. By direct fuel injection into the reactor volume, Diesel jets interaction with wall junctions of the SiC reactor significantly supports fuel distribution within the reactor volume, fuel vaporization as well as homogenization of fuel–air mixture.

The heat-release process has been compared to a free Diesel combustion indicating a significant influence of the reactor heat capacity on the thermodynamics of the process. The combustion pressure peak is significantly lowered owing to the reduced combustion temperature due to the heat accumulated in the porous reactor. This allows realizing a very low  $\text{NO}_x$ -combustion process. As already shown in the literature, this kind of internal combustion engine with heat release in porous reactor has also great potential for increasing the cycle efficiency (recuperation of heat accumulated in the reactor).

## Acknowledgments

Financial support from the Cluster of Excellence “Engineering of Advanced Materials” funded by DFG is gratefully acknowledged.

The authors thanks the Federal Ministry of Education and Research (BMBF) and German Federation of Industrial Research Asso-

ciations (AiF) for financial support of the presented investigation (Project No. 17N2207).

## References

- [1] Durst F, Weclas M. A new type of internal combustion engine based on the porous-medium combustion technique. *J Automob Eng IMechE Part D* 2001;215:63–81.
- [2] Rojas PC, Piderit GJ, Toro P. Development of open-pore silicon carbide foams. *Key Eng Mater* 1997;132–136:1731–4.
- [3] Passalacqua E, Freni S, Barone F. Alkali resistance of tap-cast SiC porous ceramic membranes. *Mater Lett* 1998;34:257–62.
- [4] Greil P. Advanced engineering ceramics. *Adv Mater* 2002;14:709–16.
- [5] Mößbauer S, Pickenäcker O, Trimis D. Application of the porous burner technology in energy- and heat-engineering. In: *Proc. 5th int conf on techn comb. Clean environment (Clean Air V)*, Lisbon; 1999. p. 519–23.
- [6] Pickenäcker O, Pickenäcker K, Wawrzinek K, Trimis D, Pritzkow W, Müller C. Innovative ceramic materials for porous-medium burners. *Interceram* 1999;48:326–30. 424–433.
- [7] Fend T, Trimis D, Pitz-Paal R, Hoffschmidt B, Reutter O. Thermal properties. In: Scheffler M, Colombo P, editors. *Cellular ceramics: structure, manufacturing, properties and applications*. Weinheim: Wiley; 2005. p. 342–60.
- [8] Schlier L, Zhang W, Travitzky N, Cypris J, Weclas M, Greil P. Macro-cellular silicon carbide reactors for a non-stationary combustion under piston engine-like conditions. Submitted for publication in *Int J Appl Ceram Technol*; 2010. p. 1–9. doi:10.1111/j.1744-7402.2010.02591.
- [9] Weclas M, Cypris J. Combustion of Diesel sprays under real-engine like conditions: analysis of low- and high-temperature oxidation processes. ILASS – Europe 2010. 23rd Annual conference on liquid atomization and spray systems. Brno, Czech Republic; 2010.
- [10] Weclas M, Cypris. Characterization of low- and high-temperature oxidation processes under non-premixed Diesel-engine like conditions. Accepted for publication in *Int J Eng Res*, in press. doi:10.1177/1468087412445682.
- [11] Weclas M, Cypris J. Combustion of Diesel spray: low- and high-temperature oxidation processes for free Diesel injection and in porous reactors. DIPSI workshop 2011 droplet impact phenomena & spray investigations. Bergamo, Italy, May 27th; 2011.
- [12] Weclas M. Some fundamental observations on the Diesel jet “destruction” and spatial distribution in highly porous structures. *J Porous Media* 2008;11(2): 125–45.
- [13] Weclas M, Cypris J. “Distribution-nozzle” concept: a method for Diesel spray distribution in space for charge homogenization by late injection strategy. ILASS – Europe 2010. 23rd Annual conference on liquid atomization and spray systems. Brno, Czech Republic; 2010.
- [14] Weclas M. Homogenization of liquid distribution in space by Diesel jet interaction with porous structures and small obstacles. 22nd European conference on liquid atomization and spray systems. Como, Italy; 2008.
- [15] Weclas M, Cypris J. Characterization of distribution nozzle operation for mixture homogenization by late diesel injection strategy. *Proc IMechE Part D J Automob Eng* 2012;226:529–46.
- [16] Weclas M. Potential of porous media combustion technology as applied to internal combustion engines. *J Thermodyn*, vol. 2010. p. 39. Article ID 789262, doi:10.1155/2010/789262.
- [17] Weclas M, Cypris J, Maksoud TMA. Thermodynamic properties of real porous combustion reactor under Diesel engine-like conditions. *J Thermodyn*, vol. 2012. p. 11. Article ID 798104, doi:10.1155/2012/798104.